03

Numerical model of heat and mass transfer and separation of the dispersed phase in high-speed dispersed-annular flows of gas and liquid

© A.G. Laptev, E.A. Lapteva

Kazan State Power Engineering University,
420066 Kazan, Russia
e-mail: tvt_kgeu@mail.ru

Received February 9, 2022
Revised April 6, 2022
Accepted April 14, 2022

To solve scientific and technical problems, physical processes are considered and systems of equations are written numerical and approximate mathematical model of combined heat and mass transfer at contact cooling of gases and heating of water, as well as turbulent transfer of particles in an ascending dispersed annular flow of gas and liquid. The numerical model is based on a system of equations in particular derivatives in two-dimensional form with boundary conditions of the fourth kind. Approximate model built using a system of algebraic equations of the cell model of the flow structure for gas and liquid phases, where the main parameters are the number of cells of complete mixing, coefficients heat and mass transfer and turbulent transfer of particles. An example of solving a system of equations is shown cell model with calculation of gas and liquid temperature profiles, moisture and particle concentrations, and also the efficiency of the heat and mass transfer process, the efficiency of separation of the finely dispersed phase from the gas liquid film in cocurrent flow. Comparative characteristics of film devices are given. Noted introduction of scientific and technical developments in the purification of natural gas at production sites.

Keywords: heat and mass transfer, gas cooling, particle separation, phase co-current flow, systems of transfer equations.

DOI: 10.21883/TP.2022.09.54675.29-22

Introduction

Mathematical modeling of transport phenomena in two-phase media has both theoretical significance in scientific research and applied in various industries. Academicians of the USSR Academy of Sciences N.N. Semenov, S.S. Kutateladze, N.M. Zhavoronkov, R.I. Nigmatulin and many of their students were among the first researchers of high-speed flows of liquid films together with a gas or vapor flow. Scientific and practical interest in technical devices of gas-liquid contact is due to the search for ways to intensify transport phenomena in two-phase media in various apparatuses and technical devices [1–4].

Cooling and purification from the dispersed phase of flue and process gases is an important problem for the enterprises of the petrochemical complex and thermal power plants (TPP). The cooling of gases is more often organized in direct contact with a liquid, more often with cold water. Spray, film and packed scrubbers are used with countercurrent phases, as well as vortex various types of interaction. From the point of view of the driving force of heat transfer, scrubbers with countercurrent phase interaction are most preferred. Purification of gases from various types of dispersed phases (solid and liquid aerosol particles and drops) at thermal power plants takes place in electrostatic precipitators, shock-inertial traps, and also in wet cleaning devices.

When cooling and cleaning relatively small volumes of gases (up to 50−60 t/h and water flow rates up to 200 t/h) and in the absence of significant restrictions on the hydraulic resistance of the scrubber, it is possible to use the mode of intensive interaction of gas and liquid in an axisymmetric or swirling dispersed-annular flow in cylindrical channels in parallel-current flow mode at gas velocity 10−45 m/s [5–9]. Due to the high-speed flow, small weight and size characteristics of the scrubber are achieved in comparison, for example, with packed ones. With the same scrubber diameter, the productivity of channels with high-speed dispersed-annular flows is 6−8 times higher than traditional packed scrubbers. The high-speed flow provides not only gas cooling, but also significant efficiency (up to 99.99%) of gas purification from the dispersed phase. The dispersed phase can be both solid particles and small droplets that form aerosol systems [8–10]. Contact tubes can be made with a rough surface and with strip swhirlers, which increases the efficiency of transfer phenomena [11–14].

The flow diagram of gas and liquid in the contact channel is shown in Fig. 1 [14].

Known mathematical models of such processes involve numerous experimental studies of both heat and mass transfer and separation of the dispersed phase, together with the study of the hydrodynamic laws of motion and interaction of gas and liquid phases [15–18]. Therefore, it seems appropriate to develop a mathematical model with a minimum amount of experimental information, the main

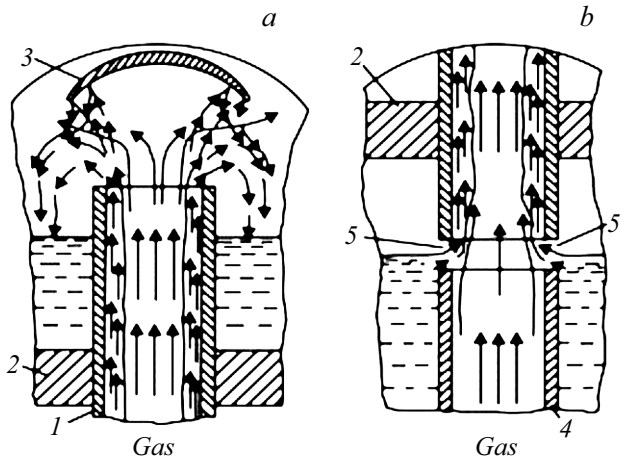

Figure 1. Film apparatus with upward movement of liquid: *a* — diagram of the movement of phases at the outlet of the pipes; *b* — scheme of phase movement at the pipe inlet; *1* — pipes, *2* — tube plates, *3* — splash guards, *4* — manifolds, *5* — slots for water supply.

of which is the hydraulic resistance of gas-liquid contact devices. This significantly reduces the time and cost of developing new technical devices for heat and mass transfer and separation of the dispersed phase.

The process of ascending motion of gas and liquid film in a contact tube of small internal diameter ($d = 0.015-0.021$ m) and height up to 1.0 m is considered. There can be several tens or even hundreds of such tubes, depending on the flow rates of the phases in the apparatus. For example, if the casing diameter of the apparatus is $D_{\text{casing}} = 1.2$ m, the number of tubes with an inner diameter of 0.021 m — 1084 pcs. The ascending regime begins at the gas velocity in the tube $w_{\text{g}} > (8-10)$ m/s (under normal conditions) and is called the strong phase interaction regime [6,7]. This process occurs when the tangential friction stress τ_{g-l} [Pa] at the gas-liquid interface is significantly greater than $\tau_w (\tau_{\text{gl}} \gg \tau_w)$ of the gravitational current $\tau_w = \rho_1 g \delta_f$ [Pa], i.e. without gas impact, where δ_f — average film thickness, [m]; ρ_1 — fluid density, [kg/m^3].

The problem of studying the phenomena of transfer during contact cooling of gases and heating of liquids (more often water), as well as gas purification from a finely dispersed phase, is being solved. The gas phase can be flue gas or process gas. Such tasks are relevant when technical solutions are required for a compact design of the apparatus and when there are no significant restrictions on the pressure drop.

Both numerical and approximate methods can be used to study conjugate heat and mass transfer and separation of the dispersed phase in a dispersed-annular flow in a contact tube. The purpose of this work is to apply these methods to simulate the phenomena of heat and mass transfer and to determine the heat and mass transfer efficiency of the process for various design and operating parameters of a dispersed-annular flow, as well as to simulate the separation of the dispersed phase by a liquid film in the problems of developing gas cleaning devices at industrial enterprises.

1. Numerical model

The theoretical basis of numerical methods are systems of differential equations of transport phenomena with partial derivatives, which are solved with the assignment of boundary conditions of various kinds [12].

The stationary turbulent motion of an ascending gas-liquid flow is considered, when the liquid phase is distributed mainly in the form of a film along the channel wall, and moves axisymmetrically in the center into the gas with a dispersed phase (particles) (Fig. 2).

Momentum, mass, and energy (heat) are exchanged through the interfacial surface of the film. The mass in this case is moisture, which in small concentrations is almost always present in the gas phase, and the dispersed phase. Condensation cooling of the gas occurs, which in some cases can provide cooling below the dew point. The liquid phase provides heat recovery of the gas phase. Heat exchange through the walls of the contact tube with the environment is insignificant. The gas phase contains small solid particles and liquid droplets, which can break off from the crests of the film waves. However, due to their low concentration, their influence on heat and mass

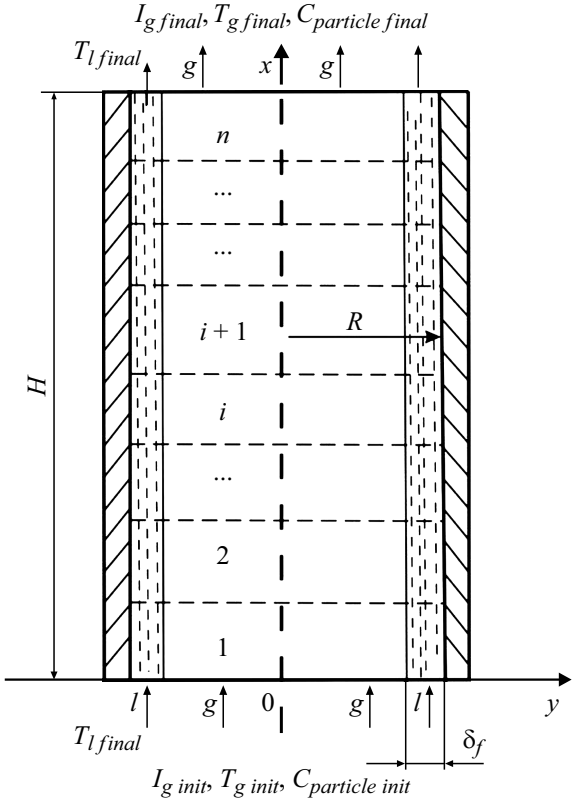

Figure 2. Scheme of gas and liquid flows in ascending forward flow and conditional division of the tube into cells.

transfer is insignificant. Taking into account that the length of the tube H is much greater than its diameter ($H \gg d$), the differential equations for the transfer of heat, mass of moisture, and dispersed particles can be written in two-dimensional form as follows:

– heat transfer in the gas phase

$$w_{\mathrm{g}}(y)\rho_{\mathrm{g}}\frac{\partial I_{\mathrm{g}}}{\partial x} = \frac{\partial q_{\mathrm{g}}}{\partial y}, \quad I_{\mathrm{g}} = f(T_{\mathrm{g}}, C_{\mathrm{g}}), \tag{1}$$

– moisture mass transfer

$$w_{\mathrm{g}}(y)\frac{\partial C_{\mathrm{g}}}{\partial x} = \frac{\partial j_{\mathrm{g}}}{\partial y}, \tag{2}$$

– heat transfer in a film

$$\rho_1 c_{\mathrm{p1}} u_1(y)\frac{\partial T_1}{\partial x} = \frac{\partial q_1}{\partial y}, \tag{3}$$

– transfer of the dispersed phase in the gas phase

$$w_{\mathrm{g}}(y)\frac{\partial C_{\mathrm{particle}}}{\partial x} = \frac{\partial j_{\mathrm{particle}}}{\partial y}. \tag{4}$$

Heat flow in the gas phase due to convection and moisture condensation

$$q_{\mathrm{g}} = (\lambda_{\mathrm{g}} + \lambda_{\mathrm{tg}})\frac{\partial T_{\mathrm{g}}}{\partial y} + I_{\mathrm{vap}}(D_{\mathrm{g}} + D_{tg})\frac{\partial C_{\mathrm{g}}}{\partial y}; I_{\mathrm{vap}} = c_{\mathrm{p1}}T_1 + r. \tag{5}$$

In expression (5), the first right term — heat transferred due to phase contact by molecular and turbulent mechanisms, and the second — heat transferred by moisture condensation, where I_{vap} is the specific enthalpy of vapor, [J/kg], at liquid temperature T_1, [°C].

Mass flow of moisture in the gas phase

$$j_{\mathrm{g}} = (D_{\mathrm{g}} + D_{\mathrm{tg}})\frac{\partial C_{\mathrm{g}}}{\partial y}. \tag{6}$$

Heat flow in the liquid phase

$$q_1 = (\lambda_1 + \lambda_{\mathrm{t1}})\frac{\partial T_1}{\partial y}. \tag{7}$$

Flow of particles in the gas phase [10]

$$j_{\mathrm{particle}} = (D_{\mathrm{particle}} + D_{\mathrm{t\,particle}})\frac{\partial C_{\mathrm{particle}}}{\partial y} - u_t C_{\mathrm{particle}}(y). \tag{8}$$

In expressions (1)–(8): x, y — longitudinal and transverse coordinates, [m]; $w_{\mathrm{g}}(y)$, $u_1(y)$ — gas and liquid velocities as functions of the transverse coordinate, [m/s]; I_s — gas enthalpy, [J/kg]; T_{g}), T_1 — gas and liquid temperatures, [°C]; C_{g} — moisture concentration, [kg/m^3]; C_{particle} — concentration of particles, [kg/m^3]; c_{pl} — specific heat capacity of liquid, [J/(kgK)]; λ_1, λ_{m1} — coefficients of molecular and turbulent thermal conductivity in the gas phase, [W/(m·K)]; λ_{g}, λ_{tg} — coefficients of molecular and turbulent thermal conductivity in the liquid phase (in a film), [W/(m·K)]; D_{g}, D_{tg} — coefficients of molecular and turbulent diffusion of moisture in the gas phase, [m^2/s]; r — specific heat of vaporization, [J/kg]; u_t — velocity coefficient of turbulent transfer of particles, [m/s]; D_{particle}, $D_{\mathrm{t\,particle}}$ — coefficients of Brownian and turbulent particle diffusion, [m^2/s]; ρ_{g} — gas density, [kg/m^3].

On the right side of expression (8), the term $u_t C_{\mathrm{particle}}(y)$ takes into account the turbulent-inertial mechanism of particle transfer [10].

The following boundary conditions are set for the system of equations (1)–(3):

for $x = 0$ (input):

$I_{\mathrm{g}} = I_{\mathrm{g\,init}}$, $T_1 = T_{\mathrm{1init}}$, $G_{\mathrm{g}} = C_{\mathrm{g\,init}}$, $C_{\mathrm{particle}} C_{\mathrm{particle\,init}}$;

for $y = 0$ (on the wall):

$\partial T_1/\partial y = 0$;

for $y = R$ (on the axis of symmetry):

$\partial I_{\mathrm{g}}/\partial y = \partial C/\partial y = \partial C_{\mathrm{particle}}/\partial y = 0$,

at $y - R - \delta_f$ (on the interface):

$q_{\mathrm{g}} - q_1$; $T_{\mathrm{g}} = T_1$; $D_{\mathrm{g}}\partial c/\partial y = \beta_{\mathrm{g}}(C - C^*)$,

$j_{\mathrm{particle}} = u_t C_{\mathrm{particle}}$,

where R — tube radius, [m]; β_{g} — mass transfer coefficient in the gas phase, [m/s]; indexes: init — initial value; * — equilibrium value. In equation (1), the enthalpy

$$I_{\mathrm{g}} = (c_{\mathrm{pg}} + c_{\mathrm{p\,vap}}\bar{C}_{\mathrm{g}})T_{\mathrm{g}} + r\bar{C}_{\mathrm{g}},$$

where $c_{\mathrm{pg}}, c_{\mathrm{p\,vap}}$ — specific heat capacities of dry gas and steam, [J/kgK]; in this expression for enthalpy I_{g}, the moisture content dimension is $\bar{C}_{\mathrm{d}}$ kg/kg.

The velocity profiles $w_{\mathrm{g}}(y)$ and $u_1(y)$ after the hydrodynamic stabilization section are usually specified as logarithmic or power-law. The coefficients of turbulent exchange in the gas phase and, especially, in a turbulent film have a complex nature of dependence on the transverse coordinate and hydrodynamic characteristics of the motion of the gas and liquid phases. Therefore, the solution of the system of equations (1)–(3) with the presented boundary conditions has certain difficulties and is more often used for research purposes. Approximate mathematical models and methods are used in practical calculations for the modernization or design of heat and mass transfer industrial apparatuses.

2. Approximate model

In approximate modeling, we will take a cell model with a conditional division of the contact tube in height into cells of complete mixing of the same size. The number of cells depends on the structure of liquid and gas flows. Let us write the equation for the heat balance of the cell model in the form

$$Q_i = Lc_{\mathrm{p1}}(T_{i,1} - T_{i-1,1}) + Q_{i,\mathrm{evap}} = KF_i(T_{1,\mathrm{g}} - T_{i,1}) + I_{\mathrm{vap}}\beta_{\mathrm{g}}F_i(C_{i,\mathrm{g}} - C^*_{i,\mathrm{g}}), \quad i = 1, 2, \ldots, n, \tag{9}$$

where Q_i — heat flow in the cell, [W]; $Q_{i,\mathrm{evap}}$ — heat flow with evaporated liquid, [W]; K — heat transfer coefficient, [W/(m^2·K)], which is equal to the heat transfer

coefficient α_g in the gas phase, $K = \alpha_{|textyg}$ since the main heat transfer resistance is concentrated in the gas phase; F_i — interfacial area, [m^2]; ($F_i = \pi(d - 2\delta_f)H/n$, H — tube height, [m]); n — number of cells; I_{vap} — vapor enthalpy, [J/kg]; $C^*_{i,g}$ — moisture content of saturated gas, [kg/m^3].

The right side of expression (9) can be written using the Lewis analogy, and then we get [15] $Q_i = F_i\beta_x(I_{i,g} - I^*_{i,g})$. For a cell, the heat flow (9) will take the form

$$Q_i = Lc_{p1}(T_{i,1} - T_{i-1,1}) + Q_{i,evap} = F_i\beta_x(I_{i,g} - I^*_{i,g}),\ i = 1, 2, \ldots, n, \quad (10)$$

where β_x — mass transfer coefficient related to moisture content difference, k[g/(m^2·s)] [19]; $I^*_{i,g}$ — enthalpy at the phase boundary at $T_{i,1}$, [°C].

Expression (10) is solved together with the heat balance equation

$$Q_i = Lc_{p1}(T_{i,1} - T_{i-1,1}) + Q_{i,evap} = G(I_{i-1,g} - I_{i,g}),\ i = 1, 2, \ldots, n, \quad (11)$$

where L, G — mass flow rates of liquid and gas, [kg/s] (assumed to be constant along the tube height); c_{p1}, c_{pg} — specific heat capacities of liquid and gas, [J/(kg·K)]. The value of $Q_{i,evap}$ is no more than 1–2% of Q_i and therefore the flow $Q_{i,evap}$ can be neglected.

Equation for moisture mass flow, [kg/s] per cell

$$M_{i,g} = \frac{G(C_{i-1,g} - C_{i,g})}{\rho_g} = \beta_g F_i(C_{i,g} - C^*_{i,g}),\quad i = 1, 2, \ldots, n. \quad (12)$$

Mass flow [kg/s] of particles deposited on the surface of the liquid film in the cell

$$M_{i,particle} = \frac{G(C_{i-1,particle} - C_{i,particle})}{\rho_g} = u_t F_i C_{i,particle},\ i = 1, 2, \ldots, n. \quad (13)$$

The coefficients of heat transfer α_g, mass transfer β_g, β_x and turbulent transport of particles u_t are taken average over phase contact surfaces and are calculated from the expressions of the mathematical model, where the main information about the modeling object is the hydraulic resistance of the contact devices [13,20]. With a significant change in the thermophysical properties of gas and liquid along the height of the contact tube, the calculation of β_g, β_x and u_t can be performed cell by cell.

The Sherwood number for a strong interaction of a gas with a liquid film is calculated by the expression [20]:

$$Sh_g = \frac{Re_g Sc_g^{0.33}\sqrt{\xi/8}}{13.73 + 2.5\ln(8.33 \cdot 10^{-3} Re_g\sqrt{\xi/8})}, \quad (14)$$

where $Sh_g = \beta_g(d - 2\delta_f)/D_g$ — Sherwood number; $Re_g = w_g(d - 2\delta_f)/\nu_g$ — Reynolds number; $Sc_g = \nu_g/D_g$ — Schmidt number; w_g — average gas velocity in the tube, [m/s]; ξ — coefficient of hydraulic resistance of gas-liquid medium. Mass transfer coefficient $\beta_x = \rho_g\beta_g$, [kg/m^2·s].

The dimensionless velocity of turbulent transport and settling of particles $u_t^+ = u_t/u_*$ is found from an expression generalizing a large number of experimental data in tubes at a gas velocity $w_g = 5-50$ m/s for aerosol particles [10] ($\tau^+ < 26.6$),

$$u_t^+ = 7.25 \cdot 10^{-4}\left(\frac{\tau^+}{1 + \omega_E\tau_r}\right)^2, \quad (15)$$

where $\tau^+ = \tau_r u_*^2/\nu_g$ — is the dimensionless relaxation time; $\tau_r = d^2_{particle}\rho_{particle}/(18\rho_g\nu_g)$ — particle relaxation time, [s]; $d_{particle}$ — particle diameter, [m]; $\omega_E = u_*/(0.05d)$ — energy-intensive pulsation frequency, [s^{-1}]; $u_* = W_g\sqrt{\xi/8}$ — dynamic velocity in the boundary layer in the gas phase at the interface, [m/s].

For $\tau^+ > 26.6$, we get [10] $U_t^+ = 0.2$.

Thus, four equations (10)–(13) are written with four unknown quantities $T_{i,1}$, $I_{i,g}$, $C_{i,g}$, $C_{i,particle}$, where the kinetic characteristics of transport phenomena are calculated by expressions (14), (15).

For the convenience of solving this system of equations, from expression (10) we write

$$T_{i,1} = T_{i-1,1} + \frac{F_i\beta_x}{Lc_{p1}}(I_{i,g} - I^*_{i,g}),\ i = 1, 2, \ldots, n. \quad (16)$$

From expression (11)

$$I_{i,g} = I_{i-1,g} - \frac{Lc_{p1}(T_{i,1} - T_{i-1,1})}{G},\ i = 1, 2, \ldots, n. \quad (17)$$

From expression (12)

$$C_{i,g} = \frac{C_{i-1,g} + \rho_g\beta_g F_l C^*_{i,g}}{I + \rho_g\beta_{gh}F_i/G},\ i = 1, 2, \ldots, n. \quad (18)$$

From expression (13)

$$C_{i,particle} = \frac{C_{i-1,particle}}{1 + \rho_g u_t F_i/G},\ i = 1, 2, \ldots, n, \quad (19)$$

where for $i = 1$ the gas and liquid inlet is in the lower part of the contact device: $T_{o1} = T_{init\,1}$; $I_{og} = I_{init\,g}$; $C_{og} = C_{init\,g}$; $C_{o\,particle} = C_{init\,particle}$. $I_{init\,g} = (c_{init,p\,g} + c_{inin,p\,vap}C_{init\,g})T_{init\,g} + rC_{init\,g}$; ($C_{init\,g} \sim$ kg/kg).

When $i = n$, the gas and water outlet is in the upper part of the contact device, where the values take on finite values.

The number of cells nn is calculated with the known Peclet (Bodenstein) number of the flow structure, with Pe = 2–10, $n = (Pe + 1.25)/2.5$, with Pe > 10, $n \approx Pe/2$. The Peclet number is calculated using semi-empirical expressions [13,14]. Moreover, the number of cells in the gas and liquid phases does not match and a smaller value is chosen. Considering that the main resistance to transport phenomena is concentrated in the

gas phase, the Taylor expression can be used in the form $\mathrm{Pe} = 0.43H/[(d - 2\delta_f)\sqrt{\xi}]$.

Thus, the profiles of liquid temperature $T_{i,1}$, gas enthalpy $T_{i,\mathrm{g}}$ and moisture content $C_{i,\mathrm{g}}$ by cells are found from the solution systems of equations (16)–(18), where all kinetic characteristics and the number of cells are determined. From solution (19), the particle concentration profile is calculated. For $i = n$ we have the values $T_{\mathrm{final}\,1}$, $I_{\mathrm{final\,g}}$, $C_{\mathrm{final\,g}}$, $C_{\mathrm{final\,particle}}$ this makes it possible to write the efficiency of transfer phenomena as the ratio of the achieved values to the maximum possible ones.

Thermal efficiency of gas cooling

$$E_g = \frac{I_{\mathrm{init\,g}} - I_{\mathrm{final\,g}}}{I_{\mathrm{init\,g}} - I^*_{\mathrm{final\,g}}}. \tag{20}$$

Thermal efficiency of water heating

$$E_1 = \frac{T_{\mathrm{final}\,1} - T_{\mathrm{init}\,1}}{T_{\mathrm{init\,g}} - T_{\mathrm{init}\,1}}. \tag{21}$$

Moisture Condensation Efficiency

$$E_c = \frac{C_{\mathrm{init\,g}} - C_{\mathrm{final\,g}}}{C_{\mathrm{init\,g}} - C^*_{\mathrm{final\,g}}}. \tag{22}$$

Particle Separation Efficiency

$$\eta = \frac{C_{\mathrm{init\,particle}} - C_{\mathrm{final\,particle}}}{C_{\mathrm{init\,particle}}}. \tag{23}$$

From the heat balance equation

$$Lc_{\mathrm{p1}}(T_{\mathrm{final}\,1} - T_{\mathrm{init}\,1}) = G(I_{\mathrm{init\,g}} - I_{\mathrm{final\,g}}), \tag{24}$$

as well as expressions for the thermal efficiency (20) and (21) follows the relation

$$\frac{E_{\mathrm{g}}}{E_1} = \frac{Lc_{\mathrm{p1}}(T_{\mathrm{final}\,1} - T_{\mathrm{init}\,1})}{G(I_{\mathrm{init\,g}} - I^*_{\mathrm{final\,g}})}. \tag{25}$$

Thus, depending on the conditions of the gas cooling and liquid heating problem being solved, by setting one of the required efficiencies (for example, E_{g} (20)), one can determine the efficiency liquid phase heating.

3. Calculation result

Figure 3 shows the results of calculations using expression (19) for the concentration profile of uranine particles in the air with a diameter of $d_{\mathrm{particle}} = 9\,\mu$m along the vertical coordinate of a dry channel with a diameter of $d = 15.75$,mm and length $H = 4.5$ m at air speed $w_{\mathrm{g}} = 18.1$ m/s and comparison with experimental data [21] (logarithmic y-axis). The experimental value is $C_{\mathrm{final}} = 1.0\%$ of the input ($\eta = 0.99$), and the calculated value is 1.3% ($\eta = 0.987$). The dynamic velocity in a dry channel with particles deposited on the surface (absolutely absorbed walls [10]) was calculated by the expression $u_* = w_{\mathrm{g}}\sqrt{\xi_{\mathrm{roug\ h}}/8}$, where

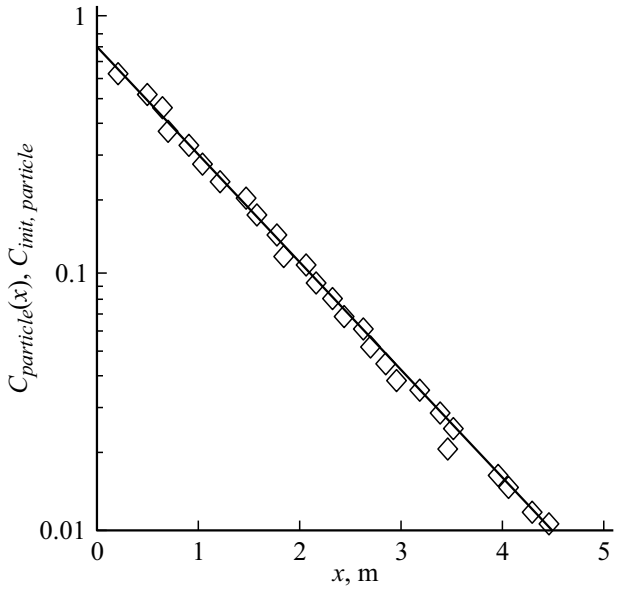

Figure 3. Concentration field of aerosol particles of uranine: rhombuses — experiments by G.A. Sehmel [21], calculation by equation (19). Particle diameter 9 μm, gas velocity 18 m/s, tube diameter 0.01575 m. Rectangles — experimental data [21].

$\xi_{\mathrm{roug\ h}}$ — is the coefficient of hydraulic resistance of the rough channel due to the dispersed phase deposited on the surface. Satisfactory agreement between the calculated and experimental profiles $C_{\mathrm{particle}}(x)/C_{\mathrm{particle\,init}}$ confirms the adequacy of the mathematical model. The discrepancy in the final concentration is not more than 1%.

For an ascending dispersed-annular flow, calculations were performed at a gas velocity $w_{\mathrm{g}} = 20$ m/s, a specific water flow rate of 2.75 m^3/(m^2·h); $T_{\mathrm{init\,g}} = 90°$C; $T_{\mathrm{init}\,1} = 20°$C; $C_{\mathrm{init}} = 0.176$ kg/kg; $I_{\mathrm{init\,g}} = 156 \cdot 10^3$ J/kg. Tube inner diameter $d = 0.0168$ m, tube length $H = 0.5$ m. Pressure drop $\Delta P = 3750$ Pa, drag coefficient $\xi = 0.525$.

As a result of solving the system of equations (16)–(18), the thermal efficiency in the gas phase is $E_{\mathrm{g}} = 0.82$. Also, for similar conditions, the calculation of the concentration profile (19) of fine particles with a diameter of 3 and 1 μm and density $\rho_{\mathrm{particle}} = 2 \cdot 10^3$ kg/m^3. For particles with a diameter of 3 μm, $\eta = 0.997$ was obtained, for particles with a diameter of 1 μm $\eta = 0.0.756$. Thus, for the given conditions, particles with a diameter of 3 μm and more are captured almost completely, and at $d_{\mathrm{particle}} < 3\,\mu$m the efficiency is significantly reduced. The results of the calculation of the mass transfer efficiency E_c (22) (air humidification with water) and the separation of particles with a diameter of 1 and 3 μm with a density of $\rho_{\mathrm{particle}} = 2000$ kg/m^3 in a tube $H = 0.2$ m long and with a diameter of$d = 0.0168$ m with an experimental pressure drop ΔP for the air–water are given in the table. For very small particles, it is possible to increase the efficiency of processes by using channels with discretely rough walls or swirling flows.

Hydraulic, mass transfer and separation characteristics during the upward axial movement of the dispersed-annular flow in a tube $H = 0.2$ m long, $d = 0.0168$ m inner diameter for the air-to-water system ($T_g \approx T_1 = 20^\circ$C) at various gas velocities and irrigation density

№	w_g, m/s	ΔP, Pa	q, m^3/(m·h)	ξ	E_c	η	
						1 μm	3 μm
1	14.7	600	0.493	0.389	0.450	0.035	0.308
2	25.5	1030	0.493	0.222	0.372	0.076	0.748
3	32.8	1550	0.493	0.202	0.349	0.156	0.74
4	38.6	1950	0.493	0.183	0.331	0.222	0.725
5	45.7	2550	0.493	0.171	0.318	0.339	0.716
6	14.7	900	1.137	0.583	0.472	0.226	0.844
7	25.3	1550	1.137	0.339	0.40	0.428	0.797
8	32.5	2150	1.137	0.285	0.370	0.61	0.772
9	38.2	2750	1.137	0.263	0.355	0.752	0.762
10	45.7	3750	1.137	0.251	0.341	0.765	0.765
11	14.6	1350	2.398	0.887	0.498	0.468	0.546
12	25.1	2450	2.398	0.544	0.427	0.771	0.836
13	32.1	3550	2.398	0.482	0.424	0.82	0.82
14	37.6	4350	2.398	0.431	0.386	0.81	0.81
15	44.6	5400	2.398	0.380	0.367	0.81	0.81

In a channel with a rough wall, the efficiency increases by 15–20%, and with band swirlers by 25–30% relative, i.e. the values $\eta = 0.85$–0.95 are achieved for particles 1 μm at channel length $H = 0.2$ m.

It follows from the calculations that at $\tau^+ < 16.6$, with an increase in the gas velocity and a constant specific water consumption, the separation efficiency increases. At $\tau^+ > 16.6$, when u_t ceases to depend on the particle diameter ($u_t = 0.2u_*$), the separation efficiency becomes constant (see table lines № 9, 10, 13–15).

Figure 4 shows the results of separation efficiency calculations for particles with diameters of 1 and 3 μm ($\rho_{\text{particle}} = 2000$ kg/m^3) at gas velocity $w_s = 32.8$ m/s and irrigation density $q = 0.493$ m^3/(m·h) (see table, line № 3) depending on the length of the channel. At $H = 1.0$ m particles with a diameter of 1 μm are captured by 90%, and with a diameter of 3 μm — 99.1%. With an increase in the specific water consumption $q > 1.0$ (m^3/m·h), the efficiency increases significantly. For example, for $w_G = 32.1$ m/s, $q = 2.398$ m^3/(m·h) (line № 13 in table) efficiency of 99.9% separation of particles with a diameter of 1–3 μm is achieved with a channel length of $H = 0.8$ m.

The heat and mass transfer efficiency of gas cooling also increases with increasing the channel length. However, in contrast to the separation efficiency η, with an increase in the gas velocity and at a constant irrigation density, the efficiency of moisture transfer E_c decreases (see the table) (a similar relationship has been established for E_g). When the gas velocity is tripled, the efficiencies E_c and E_g decrease by 30%.

The decrease in heat and mass transfer efficiency with an increase in gas flow (and gas velocity, respectively) is

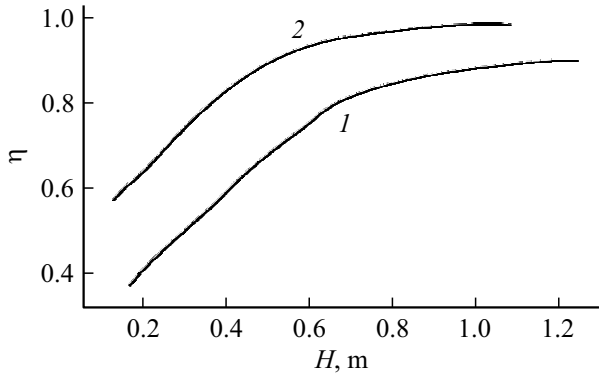

Figure 4. Dependence of particle separation efficiency (23) on the channel length. Gas velocity $w = 32.8$ m/s; irrigation density $q = 0.493$ m^3/(m · h), tube diameter $d = 0.0268$ m. *1* — particles with a diameter of $d_{\text{particle}} = 10^{-6}$, m, *2* — $d_{\text{particle}} = 3 \cdot 10^{-6}$, m.

explained by the equation of mass transfer (and heat transfer) in the form $M = G(C_{g\,\text{init}} - C_{g\,\text{final}}) = \beta_g F \Delta C$, hence $F = G(C_{g\,\text{init}} - C_{g\,\text{final}})/\beta_g \Delta C$, where ΔC — is the average driving force of mass transfer, [kg/m^3]. With an increase in gas flow, the numerator increases to the first power, and the denominator to the power of 0.75 and the required surface F increases, which characterizes the decrease in efficiency.

When separating aerosols, we write the mass flow

$$M_{\text{particle}} = G(C_{\text{particle init}} - C_{\text{particle final}}) = u_t F \Delta C_{\text{particle}}$$

and surface

$$F = G(C_{\text{particle init}} - C_{\text{particle final}})\ u_t \Delta C_{\text{particle}}.$$

For fine particles u_t (15) has the dependence $u_t \sim u_*^5$, then $u_t \sim w_g^4$. As the gas velocity increases, the required separation surface area F decreases and consequently the efficiency increases. This is due to the turbulent-inertial mechanism of particle transfer [10]. For large particles ($\tau^+ > 16.6$), the dependence $u_t \sim w_\Gamma$ is almost linear, which follows from the results presented in the table.

Fig. 5 shows the dependences of the thermal efficiency (20) of flue gas cooling with water in counterflow, as well as in ascending cocurrent phases. At a gas velocity from 2.5 to 5.5 m/s, a counterflow of a film of liquid and gas occurs, and at a velocity of more than 10 m/s, an ascending forward flow occurs. It follows from the calculations that with counterflow, the thermal efficiency is in the range $E_g = 0.68$–0.75, and with upward forward flow $E_g = 0.86$–0.95 with channel length $H = 1.0$ m and the same irrigation density ($q = 0.493$ (m^3/m·h)).

At the same time, it should be taken into account that with an upward forward flow, not only an increase E_g by 25–27% is provided, but also the flue gas capacity of the channel by a factor of 6–12.

Thus, the presented numerical mathematical model makes it possible to analyze the transfer phenomena, calculate the thermal and separation efficiencies for a given temperature

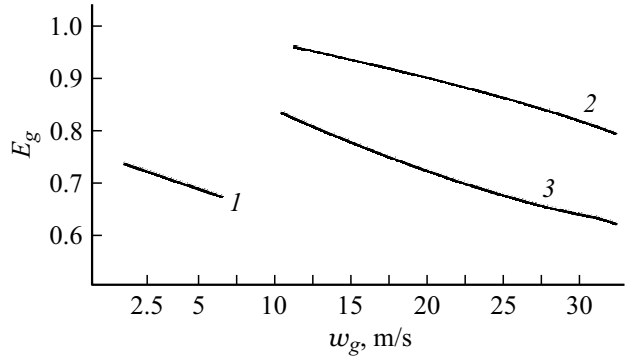

Figure 5. Dependence of the thermal efficiency of flue gas cooling ($T_{\text{ginit}} = 150^{\circ}\text{C}$) by water ($T_{\text{linit}} = 20^{\circ}\text{C}$) on average velocity gas in a channel with a diameter of $d = 0.0168$ m. *1* — counterflow of phases at weak interaction ($H = 1.0$ m), *2* — ascending forward flow of phases ($H = 1.0$ m); *3* — ascending forward flow ($H = 0.5$ m). *1–3* — irrigation density $q = 0.493\,\text{m}^3/(\text{m}\cdot\text{h})$.

regime at the inlet and phase flow rates, and as a result, select the design characteristics of an apparatus with an upward motion of a liquid and gas film in contact tubes.

Conclusion

Empirical, semi-empirical, analytical and numerical methods are used to study the phenomena of momentum, mass and energy transfer in two-phase media. All these methods, to one degree or another, have been used for many years in the development of new designs of various technical devices and technological processes. Each of the above methods has its own advantages and disadvantages. In the absence of analytical solutions, it seems appropriate to use numerical models with kinetic characteristics related to the hydraulic resistances of contact devices. It is known that the study of hydraulic resistance is much less laborious and costly.

In the work, a closed mathematical model of transfer phenomena is obtained, where the coefficients of mass transfer and turbulent transfer of a finely dispersed phase are found using the coefficient of hydraulic resistance of the gas-liquid flow in the contact tube, which significantly reduces the complexity and time of experimental studies when developing contact devices of this type. As a result of the numerical solution of the algebraic system of equations of conjugate heat and mass transfer and separation of the finely dispersed phase, the physical fields and the efficiency of the ongoing processes are calculated. This makes it possible to choose rational regime and design characteristics of contact devices under given input conditions. One of the disadvantages considered in the operation of contact devices with a gas-liquid flow at a gas velocity of more than 10 m/s is the increased value of the pressure drop and, accordingly, the power for gas supply. Therefore, it is more expedient to use such technical devices in lines with increased pressure, where there are no significant restrictions on hydraulic resistance.

The above simplified mathematical model (Section 2) is used in calculations when choosing scientific and technical solutions for natural gas separators at production sites [9,22]. The introduction of gas separators at the enterprises of „Gazprom dobycha Yamburg“ LLC shows the high efficiency of natural gas purification from various types of dispersed phase.

The presented mathematical model can be used in the range of gas velocities in the tube $w_{\text{g}} = 10-45$ m/s and irrigation density from $0.4-3.0\,\text{m}^3/(\text{m}\cdot\text{h})$ in the regime of stationary phase motion.

Funding

This study was supported by a grant from the Russian Science Foundation № 18-79-10136 (https://rscf.ru/project/18-79-10136/).

Conflict of interest

The authors declare that they have no conflict of interest.

References

[1] V.M. Kiseev, O.V. Sazhin. ZhTF, **92** (1), 22 (2022) (in Russian) DOI: 10.21883/JTF.2022.01.51847.221-21
[2] N.N. Simakov. Tech. Phys., **65** (4), (2020). DOI: 10.1134/S1063784220040209
[3] V.I. Zhukov, A.N. Pavlenko. AIP Advan., **11** (1), (2021). DOI: 10.1063/5.0023668
[4] T.R. Amanbaev. Tech. Phys., **66** (3) (2021). DOI: 10.1134/S1063784221030026
[5] R.I. Nigmatulin. *Dinamika mnogofaznykh sred* (Nauka, M., 1987) (in Russian)
[6] N.A. Voynov, N.A. Nikolayev. *Plenochnyye trubchatyye gazo-zhidkostnyye reaktory* (Otechestvo, Kazan, 2008) (in Russian)
[7] N.A. Nikolayev. *Dinamika plenochnogo techeniya zhidkosti i massoperenos v usloviyakh sil'nogo vzaimodeystviya s gazom (parom) pri odnonapravlennom voskhodyashchem ili niskhodyashchem dvizhenii* (Otechestvo, Kazan, 2011) (in Russian)
[8] M.G. Bagomedov, A.S. Pushnov Chem. Pet. Engin., **55** (5-6), (2019).
[9] A.A. Ageev, D.A. Yakhontov, T.F. Kadyrov, E.A. Lapteva, M.M. Farakhov. Vestnik tekhnol. un-ta, **24** (11), (2021) (in Russian)
[10] E.P. Mednikov. *Turbulentnyy perenos i osazhdeniye aerozoley* (Nauka M., 1980) (in Russian)
[11] N.A. Nikolayev. *Effektivnost' protsessov rektifikatsii i absorbtsii v mnogostupenchatykh apparatakh s pryamotochnovikhrevymi kontaktnymi ustroystvami* (Otechestvo, Kazan, 2011) (in Russian)
[12] L.P. Kholpanov, V.YA. Shkadov. *Gidrodinamika i teplomassoobmen s poverkhnost'yu razdela* (Nauka, M., 1990) (in Russian)

[13] A.G. Laptev, M.M. Basharov., Ye.A. Lapteva, T.M. Farakhov. *Modeli i effektivnost' protsessov mezhfaznogo perenosa* (Tsentr innovatsionnykh tekhnologiy, Kazan, 2020), 565 p. (in Russian)
[14] YU.A. Komissarov, L.S. Gordeyev, D.P. Vent. *Protsessy i apparaty khimicheskoy tekhnologii: uchebnoye posobiye dlya vuzov* (Khimiya, M., 2011) (in Russian)
[15] K.M. Jeong, H. Kessen. Bilirgen Intern. J. Heat and Mass Transfer., (53), 2361–2368 (2010).
[16] X. Shi, Xiaojun Shi, Defu Che, Brian Agnew, Jianmin Gao. Intern. J. Heat and Mass Transfer., (54), 606–615 (2011).
[17] V.V. Bespalov, L.A. Belyaev, L.S. Kuchman. MATEC Web Conf., (91), 01003 (2017).
[18] V.I. Bespalov, D.V. Melnikov. EPJ Web Conf., (110), 01007 (2016).
[19] V.S. Ponamorenko, YU.I. Aref'yev. *Gradirni promyshlennykh i energeticheskikh predpriyatiy* (Energoatomizdat, M., 1998), 376 p. (in Russian)
[20] A.G. Laptev, E.A. Lapteva. J. Engin. Thermoph., **25** (4), (2016). DOI: 10.1134/S181023281604010X
[21] G.A. Sehmel. *Aerosol Deposition from Turbulent Airstreams in Vertical Conduits* (Pacif. orthwest Lab., BNWL-578, Richland, Washington, 1968)
[22] A.A. Ageev, D.A. Yakhontov, T.F. Kadyrov, M.M. Farakhov, M.I. Farakhov. Gazovaya promyshlennost', (**1**), 82–87 (2020). (in Russian)